Int. J. Heat Mass Transfer. Vol. 31, No. 3, pp. 647–655, 1988
Printed in Great Britain

0017–9310/88 $3.00 + 0.00
Pergamon Press plc

A weak collision of two natural-convection boundary layers

L. S. YAO

Department of Mechanical and Aerospace Engineering, Arizona State University, Tempe, AR 85287, U.S.A.

(*Received* 16 *April* 1987 *and in final form* 22 *July* 1987)

Abstract—The collision of two natural-convection boundary layers at the tip of a vertical wedge is used to demonstrate that a double-deck flow structure provides a proper description of the heat-convection mechanism which is shared by many convection problems with sudden geometry changes. The present theory differs from previous work which indicate the existence of recirculating flow regions. This difference is due to a failure to recognize that recirculating flow structures can only exist for forced flows, but not for natural-convection boundary layers or wall jets. The present solution is obtained by a proper application of Prandtl's transposition theorem for geometries with finite solid displacements and appropriately matches the upstream natural-convection boundary layers and the downstream thermal plume. The interaction of the local pressure development in the main deck (outer layer) and the displacement of the lower deck (inner layer) removes the singularity associated with the boundary-layer equations at the location where the viscous layers leave the solid surface.

1. INTRODUCTION

THE COLLISION of two boundary layers which are driven by body forces are frequently found in fluid flows. Examples include flows near the equator of a spinning sphere [1, 2], natural-convection boundary layers near the top of a blunt body [3–5] or in a cavity, and secondary boundary layers in a curved pipe [6–8], or in a heated straight pipe [9]. Since the boundary-layer equations are parabolic and are not affected by downstream activities, the collision phenomena cannot be adequately described by the boundary-layer equations alone. Independently, Messiter [10] and Smith and Duck [11] developed a double-deck theory which shows that a disturbance inside a boundary layer driven by body forces (equivalently, a flow in which the motion outside of the boundary layer is much slower than that inside) can have an upstream influence to a distance of $O(\varepsilon^{6/7})$, where $\varepsilon = Re^{-1/2}$ or $Gr^{-1/4}$; Re is the appropriate Reynolds number for forced flows and Gr is the Grashof number for natural-convection boundary layers. Messiter adopted the natural-convection boundary layer along a finite vertical flat plate as a model problem to show, by this double-deck structure, that the boundary-layer solution on the plate can smoothly join the solution of the thermal plume [12] above the plate. The structure of the double deck shares many similarities with the triple-deck structure near the trailing edge of a flat plate in a uniform stream [13, 14]. Smith and Duck were interested in developing a general theory to describe the collision of two non-parallel wall layers. They conjectured that the main boundary layer separates at a distance $O(Re^{-3/14})$ from the location of the collision and a relatively large recirculation flow exists below the main boundary layer. On the other hand, such a recirculating flow has not been identified in the numerical solution of the collision of boundary layers near the equator of a spinning sphere or in experiments of natural convection near the top of a blunt body.

The first numerical solution of a double-deck flow structure was obtained by Smith [15]. The model problem studied by Smith involved a rotating disk, a degenerate case of a rotating sphere. Two boundary layers meet at the edge of the disk and form a free-boundary flow. Since the boundary layers are parallel and do not collide, no region of recirculating flow exists. This problem shares many similarities with the problem of natural convection along a vertical finite plate [10, 16].

The results in a subsequent paper by Merkin and Smith [17] clearly cast doubt on the validity of a double-deck structure to describe the flow behavior near a geometry change. The model problem studied by Merkin and Smith is natural-convection boundary layers near a corner, or the trailing edge of a vertical wedge. They formulated the equations of a double-deck structure for corners the angles of which differed slightly from 180°, or for wedges of very small angles. Their solutions show that recirculating eddies, which are physically unrealistic and are not consistent with expectation, exist even for these two limiting cases.

In this paper, natural convection along a vertical-sharp wedge (see Fig. 1) is used to demonstrate that the double deck is indeed a proper flow structure for a weak collision of two boundary layers driven by body forces. The key step in formulating the problem is to choose a coordinate system in which regions of different physics can be properly matched. Prandtl's

NOMENCLATURE

a	constant, equation (13)
A	displacement, equations (17)
b	constant, equations (26)
f	streamfunction, equations (4)
g	gravitational acceleration
Gr	Grashof number, equations (1)
l	wedge height
k	thermal diffusivity
p	pressure
T	temperature
x, y	coordinates
u, v	velocities.

Greek symbols

α	$\tan\phi$
δ	displacement, equations (1)
ε	small parameter, equations (1)
η	boundary-layer coordinate, equations (4)
θ	dimensionless temperature, equations (1)
ν	kinematic viscosity
ρ	density
τ	shear stress
ϕ	half-wedge angle
ψ	streamfunction, equations (7).

Subscripts

b	natural-convection boundary layer
p	thermal plume
l	double deck.

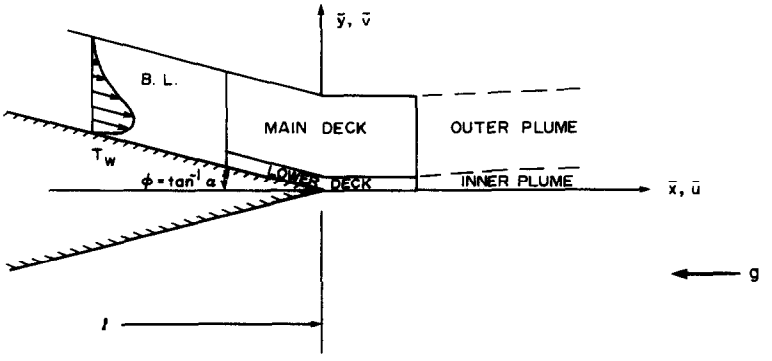

FIG. 1. Physical model and coordinates.

coordinates, as extended by Yao [18], are found to be suitable for the problem and are applied to the double-deck equations before solving them numerically. The details are described in Section 2.

Sections 3 and 4 briefly summarize the structure of the natural-convection boundary layers on the wedge, and the thermal plume above it. This establishes the notation and the required matching conditions. The double-deck equations are derived and solved in Section 5. The reason why the collision is identified as 'weak' will become clear in the conclusion section.

A proper matching principle is required if a correct matching between major regions of different physics is to be achieved. For certain problems. The importance of the existence of a double-deck solution does not rely on its contribution toward improving predictive capability in a small region. More important is the fact that the structure provides a matching principle among various regions which can occur in the flow field of many heat-transfer and fluid-mechanics problems involving large parameters without actually solving the double-deck equations. On the other hand, double decks may be the major part of the flow structure for the problem, e.g. as in impinging jets. A direct numerical solution of the Navier–Stokes equations for such problems frequently fails to provide an accurate result due to a lack of resolution in those small regions. A direct example to substantiate the above claim is the problem solved in this paper.

Another implication of the solution presented in this paper concerns the separation of a forced flow under an unfavorable pressure gradient. The separation of such a forced flow may be interpreted as the collision of two viscous layers, one driven by a forced flow and the other by an induced recirculating flow. This model is in line with the fact that Goldstein's singularity is not removable for a boundary layer driven by an adverse pressure gradient [19]. This fact, in turn, implies that the classical boundary-layer/inviscid-flow structure assumed globally does not yield a correct limiting description of the Navier–Stokes equations. Two triple decks and/or double decks may provide a proper structure with which to match a forced flow with recirculating eddies at separation. More work is required to establish a firm ground for this conjecture; however, it may provide the missing link in obtaining a solution for a large-scale separation.

2. FORMULATION

Cartesian coordinates $(\bar{x}, \bar{y})$ are used, and the corresponding velocities are $(\bar{u}, \bar{v})$. The $\bar{x}$-axis is aligned with the direction of gravity. The half-wedge angle is denoted by $\phi = \tan^{-1}\alpha$, and the height of the wedge is l. The wall temperature is held at T_w and the ambient temperature is T_∞.

The details of the extension of Prandtl's transposition theorem have been discussed by Yao [18, 20], and a brief summary is sufficient. The dimensionless variables in Prandtl's coordinates are defined by

$$\hat{x} = \frac{\bar{x}}{l}, \quad \hat{y} = \frac{\bar{y} - \bar{\delta}(\bar{x})}{l}$$

(coordinates)

$$\hat{u} = \frac{\bar{u}}{U_\infty}, \quad \hat{v} = \frac{\bar{v} - \bar{\delta}_{,\hat{x}}\bar{u}}{U_\infty}$$

(velocities)

$$\hat{P} = \frac{\bar{P} - \bar{P}_\infty}{\rho U_\infty^2}$$

(pressure)

$$\hat{\theta} = \frac{T - T_\infty}{T_w - T_\infty}$$

(temperature) (1)

$$\varepsilon^{-4} = Gr = \beta g (T_w - T_\infty) l^3 / \nu^2$$

(Grashof number)

$$U_\infty = \nu / a\, Gr^{1/2}$$

(characteristic velocity)

$$Pr = \nu / \kappa$$

(Prandtl number)

$$\hat{\delta} = \bar{\delta}/l = \alpha \hat{x} = \begin{cases} 0, & \hat{x} > 0 \\ \tan\phi\, \hat{x}, & \hat{x} < 0 \end{cases}$$

(displacement)

where the subscript after a comma denotes a derivative. The dimensionless form of the equations of continuity, motion and energy with the Boussinesq approximation for density ρ are

$$\hat{u}_{,\hat{x}} + \hat{v}_{,\hat{y}} = 0$$

$$\hat{u}\hat{u}_{,\hat{x}} + \hat{v}\hat{u}_{,\hat{y}} = -\hat{P}_{,\hat{x}} + \hat{\delta}_{,\hat{x}}\hat{P}_{,\hat{y}} + \hat{\theta} + \varepsilon^2[\hat{u}_{,\hat{x}\hat{x}} + (1+\hat{\delta}_{,\hat{x}}^2)\hat{u}_{,\hat{y}\hat{y}} - 2\hat{\delta}_{,\hat{x}}\hat{u}_{,\hat{x}\hat{y}} - \hat{\delta}_{,\hat{x}\hat{x}}\hat{u}_{,\hat{y}}]$$

$$\hat{u}\hat{v}_{,\hat{x}} + \hat{v}\hat{v}_{,\hat{y}} + \hat{\delta}_{,\hat{x}\hat{x}}\hat{u}^2 = \hat{\delta}_{,\hat{x}}\hat{P}_{,\hat{x}} - (1+\hat{\delta}_{,\hat{x}})\hat{P}_{,\hat{y}} - \hat{\delta}_{,\hat{x}}\hat{\theta} + \varepsilon^2[\hat{v}_{,\hat{x}\hat{x}} + (1+\hat{\delta}_{,\hat{x}}^2)\hat{v}_{,\hat{y}\hat{y}} - 2\hat{\delta}_{,\hat{x}}\hat{v}_{,\hat{x}\hat{y}} - \hat{\delta}_{,\hat{x}\hat{x}}\hat{v}_{,\hat{y}} + \hat{\delta}_{,\hat{x}\hat{x}\hat{x}}\hat{u} + 2\hat{\delta}_{,\hat{x}\hat{x}}\hat{u}_{,\hat{x}} - 2\hat{\delta}_{,\hat{x}}\hat{\delta}_{,\hat{x}\hat{x}}\hat{u}_{,\hat{y}}]$$

$$\hat{u}\hat{\theta}_{,\hat{x}} + \hat{v}\hat{\theta}_{,\hat{y}} = \frac{\varepsilon^2}{Pr}[\hat{\theta}_{,\hat{x}\hat{x}} + (1+\hat{\delta}_{,\hat{x}}^2)\hat{\theta}_{,\hat{y}\hat{y}} - 2\hat{\delta}_{,\hat{x}}\hat{\theta}_{,\hat{x}\hat{y}} - \hat{\delta}_{,\hat{x}\hat{x}}\hat{\theta}_{,\hat{y}}]. \quad (2)$$

In transformed space, the wedge is represented by $\hat{y} = 0$ for $\hat{x} < 0$. This substantially simplifies the numerical integration procedure in solving the above equations.

The formulation of Merkin and Smith [17] applies Prandtl's transformation to their lower-deck equations, but not to their main-deck equations. This limits the height of any geometric change to the same order as the thickness of the lower deck. In the present formulation, the lower deck is assumed to be parallel to the solid surface; therefore, it is not limited to cases of vanishingly-small wedge angles. This extension is achieved by a proper application of Prandtl's transformation to the main-deck equations. As has been discussed by Yao [18, 20], the complete set of boundary-layer equations in Prandtl's coordinates can only be obtained by transforming the Navier–Stokes equations *before* adopting the boundary-layer approximation. Important terms can be erroneously ignored if one applies Prandtl's transformation directly to the boundary-layer equations. It can be shown that, for a wedge angle of $O(\varepsilon^{3/7})$, the present formulation is almost identical to that of Merkin and Smith. The only difference is that the displacement A for the present formulation is measured from the surface of the wedge, while theirs is measured from $\bar{y} = 0$. Consequently, the difference between the two solutions in the physical space is $O(h\varepsilon^{3/7})$, where h represents the normalized solid displacement of the geometry. In other words, Merkin and Smith applied Stokes' linearization to their main-deck formulation. This limits their solution to very small h. The present solution agrees with that of Merkin and Smith in the limit $\alpha \to 0$ (a vertical flat plate [16]).

The proper equations for the natural-convection boundary layer before the collision, for the plume, and for the double deck in Prandtl's coordinates are described below. They are valid for *finite* wedge angles.

3. NATURAL-CONVECTION BOUNDARY LAYER

The scales for the natural-convection boundary layer are well known: the thickness of the boundary layer and the normal velocity are $O(\varepsilon)$. The boundary-layer coordinates are

$$x_b = 1 + \hat{x}, \quad y_b = \hat{y}/\varepsilon. \quad (3)$$

The expansions for the velocities, the pressure and the temperature are

$$\hat{u} = (1+\alpha^2)(4x_b)^{1/2} f_b'(\eta_b) + \dots$$
$$\hat{v} = -\varepsilon(1+\alpha^2)(4x_b)^{-1/4}(3f_b - \eta_b f_b') + \dots$$
$$\hat{P} = 0 + \dots$$
$$\hat{\theta} = \theta_b(\eta_b) + \dots \quad (4)$$

where subscript b is used to denote that the variables are associated with the boundary layer and $\eta_b = y_b/(4x_b)^{1/4}$. The prime denotes derivatives with respect to η_b. The substitution of equations (3) and (4) into equations (2), with terms of small orders neglected, yields the equations for the natural-con-

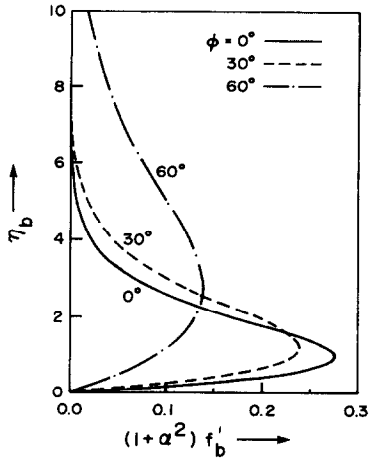

FIG. 2. Axial velocity of natural-convection boundary layer.

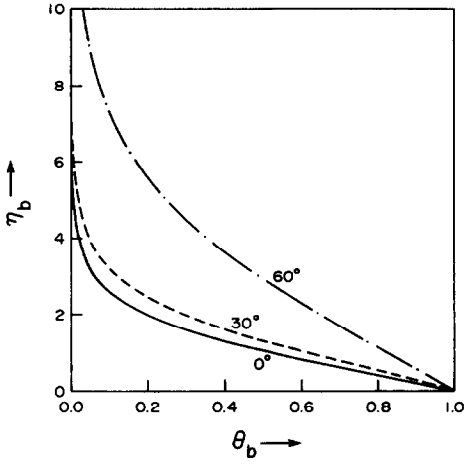

FIG. 3. Temperature distribution of natural-convection boundary layer.

vection boundary layer. They are

$$f_b''' + 3f_b f_b'' - 2f_b'^2 = -\theta_b/(1+\alpha^2)^3$$
$$\frac{1}{Pr}\theta_b'' + 3f_b\theta_b' = 0. \tag{5}$$

The associated boundary conditions are

$$\eta_b = 0, \quad f_b = f_b' = 0, \quad \theta_b = 1 \cdot$$
(wall condition)
$$\eta_b \to \infty, \quad f_b', \quad \theta_b \to 0$$
(matching with quiescent ambient). (6)

The solutions of equations (5) satisfying conditions (6) can be easily obtained by numerical integration. A typical axial velocity profile and temperature distribution are given in Figs. 2 and 3 for $\phi = 0°$, 30° and 60°, respectively. It is clear that the magnitude of the velocity decreases and the thickness of the boundary layer increases for wedges of larger angles. This is because the component of the buoyancy force parallel to the surface of the wedge decreases when the wedge angle increases. Consequently, the heat-transfer rate and wall shear are smaller for a larger-angle wedge.

In Prandtl's coordinates, the axial direction is not parallel to the surface. Thus, the axial momentum equation is the projection of the momentum equation along the solid surface onto this axis. One would expect that the solution of the axial momentum equation in Prandtl's coordinates might be restricted to the case of a small angle between the axial direction and the surface. Therefore, the natural-convection boundary-layer equations in the coordinates normal and parallel to the wedge are solved independently in order to find the restriction on Prandtl's transformation. The local wall heat flux and shear stress are compared. It is found that these two quantities, predicted by solving the equations in two different coordinate systems, agree for all wedge angles (up to 85° in our computations). However, since Prandtl's transformation is singular for a wedge with a half angle of 90° (a horizontal plane), it is reasonable to expect that the computations will become increasingly difficult as this limiting angle is approached.

4. THERMAL PLUME

An additional advantage of adopting Prandtl's coordinates is that the axial velocity of the transformed natural-convection boundary layer is in line with that of the near plume, and the two velocities can be readily matched at $\hat{x} = 0$. Consequently, the distribution of velocity and temperature inside a thermal plume for small $\hat{x}$ is essentially similar to that above a vertical plate of finite length [12], but with a different initial condition. Since its structure is also very similar to the Goldstein [19] near-wake solution behind a flat plate, Yang's solution [12] consists of two parts, an inner plume and an outer plume. The solution form is briefly outlined below.

The normal coordinate is defined as $y_p = \hat{y}/\varepsilon$ to be consistent with the fact that the plume is thin. The appropriate expansions for small y_p (inner plume) are

$$\hat{\psi} = (3\hat{x})^{2/3}\lambda_1^{1/3} f_0(\eta) + \ldots$$
$$\hat{\theta} = 1 + (3\hat{x})^{1/3}\lambda_1^{-1}\mu_1 g_0(\eta) + \ldots \tag{7}$$

where

$$\eta = \lambda_1^{1/3} y_p' (3\hat{x})^{1/3}$$
$$\lambda_1 = \sqrt{2}(1+\alpha^2) f_b'(0)$$
$$\mu_1 = \frac{1}{\sqrt{2}}\theta_b'(0)$$

and $\hat{\psi}$ is the streamfunction and is introduced to satisfy equation $(2)_1$. The governing equations for f_0 and g_0 can be obtained by substituting equations (7) into equations (2) and collecting terms of equal powers of $\hat{x}$. The result is

$$f_0''' + 2f_0 f_0''' - f_0'^2 = 0$$
$$\frac{1}{Pr} g_0'' + 2f_0 g_0' - f_0' g_0 = 0. \tag{8}$$

The prime denotes the derivative with respect to the appropriate independent variable.

The required conditions for the inner plume become:

$$\begin{aligned}&(1)\qquad \eta=0:\ \ f_0=f_0''=g_0'=0\\&\qquad\qquad\text{(symmetry condition)};\\&(2)\qquad \eta\to\infty:\ \ f_0'\to\eta+a_1\\&\qquad\qquad\qquad g_0\to\eta+a_1.\end{aligned}\tag{9}$$

The expansions for $y_p \sim O(1)$ (outer plume) are

$$\begin{aligned}\hat{\psi}&=\Psi_b(y_p)+(3\hat{x})^{1/3}\Psi_1(y_p)+\dots\\ \hat{\theta}&=\Theta_b(y_p)+(3\hat{x})^{1/3}\Theta_1(y_p)+\dots\end{aligned}\tag{10}$$

where

$$\Psi_b'=\sqrt{2(1+\alpha^2)}f_b'\quad\text{and}\quad\Theta_b=\theta_b=\theta_b(x_b=1).$$

Similarly, the governing equations for Ψ's and Θ's can be obtained from equations (10) and (2). They are

$$\begin{aligned}\Psi_b'\Psi_1'-\Psi_b''\Psi_1&=0\\ \Psi_b'\Theta_1-\Psi_1\Theta_b'&=0.\end{aligned}\tag{11}$$

The solutions of equations (11) are

$$\begin{aligned}\Psi_1&=a_1\lambda_1^{-1/3}\Psi_b'(y_p)\\ \Theta_1&=a_1\lambda_1^{-1/3}\Theta_b'\end{aligned}\tag{12}$$

in order to match with the inner plume. It is obvious that the structure of the solution for a plume above a wedge is identical to that above a vertical plate. Its solution can be found in ref. [16] and is not repeated here. Constant a_1 can be determined from the numerical solution of equations (8); the result is

$$a_1=\lim_{\eta\to\infty}[(2f_0)^{1/2}-\eta]=0.6185.\tag{13}$$

5. DOUBLE-DECK STRUCTURE

Since the y-component of the velocity in the plume is singular at $\bar{x}=0$, a double-deck structure [10, 11] is required to join the solutions of the natural-convection boundary layer and the thermal plume. The present formulation is for a finite solid displacement and has not been derived before.

We will describe the double decks. Following Messiter [10], the dimensions of the main deck are $\varepsilon^{6/7}\times\varepsilon$. The stretched coordinates become

$$\begin{aligned}x_1&=\frac{\hat{x}}{\varepsilon^{6/7}}\\ y_1&=\frac{\hat{y}}{\varepsilon}=y_b.\end{aligned}\tag{14}$$

The expansions of the dependent variables are

$$\begin{aligned}\hat{u}&=\Psi_b'(y_1)+\varepsilon^{2/7}u_1(x_1,y_1)+\dots\\ \hat{v}&=\varepsilon^{3/7}v_1(x_1,y_1)+\dots\\ \hat{p}&=\varepsilon^{4/7}p_1(x_1,y_1)+\dots\\ \hat{\theta}&=\theta_b(y_1)+\varepsilon^{2/7}\Theta_1(x_1,y_1)+\dots\end{aligned}\tag{15}$$

The equations governing the above dependent variables can be derived from equations (2). They are

$$\begin{aligned}\frac{\partial u_1}{\partial x_1}+\frac{\partial v_1}{\partial y_1}&=0\\ \Psi_b'\frac{\partial u_1}{\partial x_1}+\Psi_b''v_1&=0\\ \Psi_b'\frac{\partial v_1}{\partial x_1}&=-(1+\alpha^2)\frac{\partial p_1}{\partial y_1}\\ \Psi_b'\frac{\partial\Theta_1}{\partial x_1}+\Theta_b'v_1&=0.\end{aligned}\tag{16}$$

The solutions of the above equations can be expressed as

$$\begin{aligned}u_1&=\Psi_b''(y_1)A_1(x_1)\\ v_1&=-\Psi_b'(y_1)A_1'(x_1)\\ p_1&=-\frac{A''(x_1)}{1+\alpha^2}\int_{y_1}^{\infty}\Psi_b'(y_1)^2\,dy_1\\ \Theta_1&=\Theta_b'(y_1)A_1(x_1).\end{aligned}\tag{17}$$

The above equations show that A_1'' is not continuous at $x_1=0$, but that A_1 and A_1' are continuous. This implies that u_1 and v_1 are continuous at $x_1=0$. Consequently, the normal velocity in physical space is not continuous due to the discontinuity of α (see equations (1)). Physically, this discontinuous normal velocity represents the *colliding* velocity component of the two boundary layers. The advantage of adopting the Prandtl transformation for the main deck is that the discontinuity of the colliding velocity is removed. This is the key reason why the present numerical results do not contain physically unrealistic recirculating eddies. Since the streamwise velocity component is continuous at the collision, this suggests that a 'fine' flow structure near the collision point is required to smooth out this discontinuity, but its contribution is smaller and less important to the present problem. For a collision of two asymmetric natural-convection boundary layers, the direction of the thermal plume immediately above the collision will be determined by the fine flow structure in this small region.

A lower deck is needed since solution (17) does not satisfy the wall condition on the cylinder. The thickness of the lower deck is $O(\varepsilon^{9/7})$. Therefore, $\hat{y}=\varepsilon^{9/7}\gamma^{1/7}\lambda_1^{-4/7}y$, and the expansions of the dependent variables, which match with the variables of the surrounding areas, are

$$\begin{aligned}\hat{u}&=\varepsilon^{2/7}\gamma^{1/7}\lambda_1^{3/7}u(x,y)+\dots\\ \hat{v}&=\varepsilon^{5/7}\gamma^{-1/7}\lambda_1^{4/7}v(x,y)+\dots\\ \hat{p}&=\varepsilon^{4/7}\gamma^{2/7}\lambda_1^{6/7}p(x,y)+\dots\\ \hat{\theta}&=1+\varepsilon^{2/7}\gamma^{1/7}\lambda_1^{-4/7}\mu_1\Theta(x,y)+\dots\\ A_1&=\gamma^{1/7}\lambda_1^{-4/7}A(x)\end{aligned}\tag{18}$$

where

$$x = \gamma^{-3/7}\lambda_1^{5/7}x_1$$

and

$$\gamma = \int_0^\infty \Psi_b'^2\, dy_1.$$

Substitution of equations (18) into equations (2) gives

$$\begin{aligned}
&\frac{\partial u}{\partial x}+\frac{\partial v}{\partial y}=0\\
&u\frac{\partial u}{\partial x}+v\frac{\partial u}{\partial y}=-\frac{1}{1+\alpha^2}\frac{\partial p}{\partial x}+(1+\alpha^2)\frac{\partial^2 u}{\partial y^2}\\
&\frac{\partial p}{\partial y}=0\\
&u\frac{\partial \Theta}{\partial x}+v\frac{\partial \Theta}{\partial y}=\frac{(1+\alpha^2)}{Pr}\frac{\partial^2 \Theta}{\partial y^2}.
\end{aligned} \tag{19}$$

Expansions (19) must match with the boundary-layer solution as $x \to -\infty$ so that

$$u \to y \quad \text{and} \quad \Theta \to y. \tag{20}$$

As $y \to \infty$, they must also match with the main deck

$$u \to y + A(x_1) \quad \text{and} \quad \Theta \to y + A(x_1). \tag{21}$$

On the surface of the cylinder, $y = 0$ and $x < 0$, the wall conditions are

$$u = v = \Theta = 0 \tag{22}$$

and

$$v = \frac{\partial u}{\partial y} = \frac{\partial \Theta}{\partial y} = 0 \tag{23}$$

are applied along $y = 0$ for $x > 0$. Finally, since the normal pressure gradient vanishes across the lower deck

$$p = p_1(y = 0) = \frac{-1}{(1+\alpha^2)}A''(x). \tag{24}$$

Physically, $A(x)$ represents the displacement effect of the lower deck, and can be determined from the solution of the lower deck. The main-deck solution matches with the boundary-layer solution as $x \to -\infty$ and the outer plume as $x \to \infty$. This implies that

$$A(-\infty) \to 0 \quad \text{and} \quad A(\infty) \to a_1(3x)^{1/3}. \tag{25}$$

An in-depth interpretation of $A(x)$ and its role in transmitting a disturbance upstream within these thin wall layers can be found in refs. [10, 11 16].

Since α assumes different values for $x < 0$ and $x > 0$ (see equations (1)), equations (19) must be solved separately and then matched at $x = 0$. One should note that the lower-deck solution can be obtained by marching downstream without knowing the upstream normal velocity component. Equations (24) and (25) define a two-point boundary-value problem which transmits the disturbance upstream. Special attention is required to obtain the solution of this problem. The continuity of the displacement $A(x)$ and its derivative is enforced in the numerical solution. Since the double decks provide a mechanism of viscous–inviscid interaction, this allows a large adverse pressure gradient to be established over a relatively small region. Therefore, a smooth solution can be obtained across the collision point. In other words, the catastrophe of the classical boundary-layer theory, due to Goldstein's singularity at the collision point, is avoided by the introduction of the double-deck structure.

The numerical method used to solve equations (19) is almost identical to the one used previously [16, 17]. A central-difference scheme is used for derivatives with respect to y and a backward scheme is used for x-derivatives. The grid size of 0.01 was selected after trials with values of 0.02 and 0.005. The results are believed to be accurate to the third decimal point.

For $x \to -\infty$, the solutions asymptotically approach

$$\begin{aligned}
u &\sim y + \psi'(y) b\, e^{kx}\\
v &\sim -\psi(y) b\, e^{kx}\\
p &\sim -0.8972 kb\, e^{kx}\\
A &\sim b\, e^{kx}
\end{aligned} \tag{26}$$

where $k = 0.8972(1+\alpha^2)$. $\psi(y)$ satisfies

$$\psi^{(IV)} - \frac{k}{1+\alpha^2} y\psi''' = 0 \tag{27}$$

and conditions

$$\begin{aligned}
&\text{(i)}\ \ y = 0, \quad \psi' = \psi = 0, \quad \psi''' = -0.8972^3\\
&\text{(ii)}\ \ y \to \infty, \quad \psi' \to 1.
\end{aligned} \tag{28}$$

Numerical iteration starts at a selected $x_{-\infty}$ with a guessed b. The value of b is adjusted until the boundary condition at $x_{-\infty}$ is satisfied. We found that, for large α, it is necessary to choose a smaller value of $x_{-\infty}$. This is because the range of upstream influence decreases as α increases, as indicated by equations (26).

The lower-deck displacement $A(x)$ is plotted for $\phi = 0°$, 30° and 60° in Fig. 4. The range of upstream influence decreases as ϕ increases in agreement with the asymptotic solution, equations (26). Equation (25) is also plotted in Fig. 4 to show that $A(x)$ asymptotically approaches the downstream condition for $x > 8$. For a larger ϕ, a greater distance is required for $A(x)$ to approach the result of equation (25). The induced pressure is given in Fig. 5. A favorable pressure gradient is developed along the wedge. Downstream of the wedge, the pressure starts to recover and overshoots the ambient pressure before it asymptotically returns to the ambient pressure. A stronger favorable pressure gradient for a larger ϕ is indicated by the numerical solution. It also has a higher overshoot and takes a longer distance to merge with the ambient pressure. The increase of the wall shear and the wake velocity along $y = 0$ are presented in Fig. 6. The larger shear stress at the tip of the wedge for smaller ϕ is the

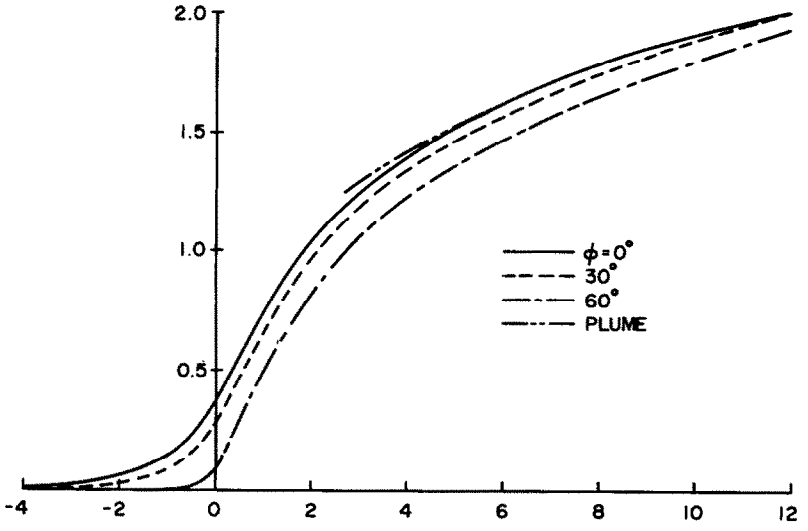

FIG. 4. Displacement $A(x)$.

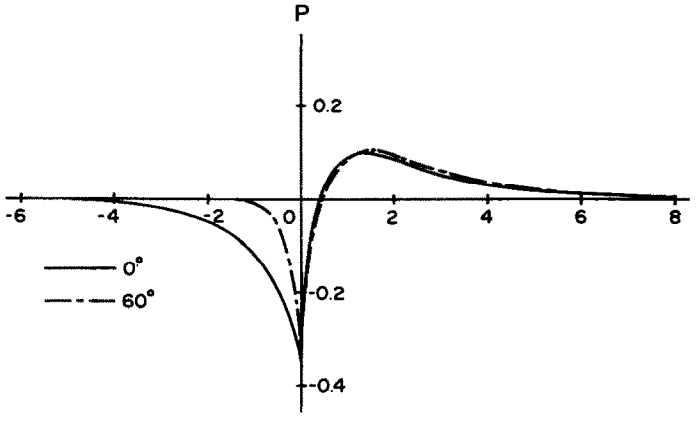

FIG. 5. Pressure distribution.

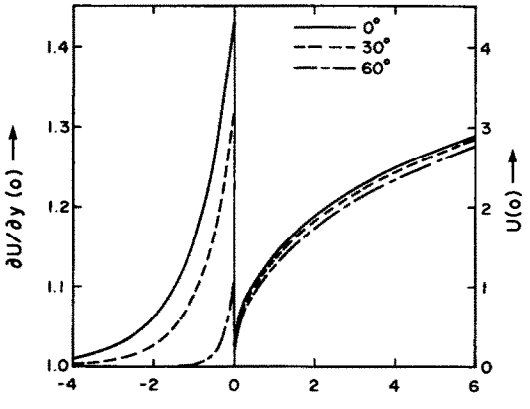

FIG. 6. Wall shear and centerline wake velocity.

consequence of the longer distance of the upstream influence. The centerline wake velocity increases more slowly for a wedge of larger angle.

It is clear that no recirculating flow has been identified by the numerical double-deck solution. This agrees with experimental observation and our expectation. It should be noted that the decreasing distance of the upstream influence of the interaction with increasing wedge angles is expected. This is a consequence of the fact that the natural-convection boundary layers become weaker for a larger wedge angle. Of course, there is no flow when the half-wedge angle becomes 90° (a horizontal plane). This rules out the possibility of using the present problem to discuss a 'head-on' collision of two boundary layers. Nevertheless, the present results suggest that the zeroth-order velocity normal to the direction of a head-on collision is zero. The collision process cancels the momentum of the colliding streams, and occurs within a shorter distance than the axial extent of a double deck. Further effort is required in order to delineate the collision flow structure. The above reduction, however, is in line with the observation of the collision of natural convection boundary layers above a horizontal cylinder [4].

The drag on one side of the wedge, obtained by integrating the perturbation of the wall shear from the boundary-layer solution, is

$$\tau = \varepsilon^{-1}(1+\alpha^2)^{1/2}[0.8\lambda_1 + \varepsilon^{6/7}\gamma^{3/7}\lambda_1^{2/7}\tau_c] \quad (29)$$

Table 1. Coefficient for wall shear

$\tan^{-1}\alpha$	λ_1	γ	τ_c
0°	0.4780	0.6528	0.4332
30°	0.3336	0.6075	0.2476
60°	0.0845	0.4616	0.2797×10^{-1}
80°	0.0011	0.1927	0.2711×10^{-4}

where

$$\tau_c = \int_{-\infty}^{0} \left(\frac{\partial u}{\partial y} - 1\right) dx.$$

The values for λ_1, γ and τ_c are listed in Table 1. The numerical solution has been obtained for ϕ up to 85°.

6. DISCUSSION AND CONCLUSION

The collision of two inclined viscous layers driven by buoyancy has been described. No recirculating eddies have been indicated, which agrees with experimental observation. The local extra wall shear stress and heat flux contribute little to the total drag and heat flux. The importance of the existence of a correct double-deck solution is not to improve the predictive capability for such complex flows. The flow structure, which describes how a viscous layer collides with another, or with a solid wall, provides a proper matching principle between two viscous layers upstream and downstream of the collision point. The solutions for these viscous layers can then be confidently calculated by a marching technique, since their governing equations are parabolic differential equations.

The double-deck solution presented in this paper indicates that the matching of a downstream viscous layer with an upstream layer can be simply achieved by aligning them. This is how the natural-convection boundary layer along a wedge provides an initial condition for the downstream plume. It is believed that the same matching principle can be applied to other flows.

The collision is called *weak* because the flow model adopted in the paper cannot be extended to a head-on collision. Further study is required to understand the flow structure in a head-on collision.

REFERENCES

1. L. Howarth, Note on the boundary layer on a spinning sphere, *Phil. Mag.* **42,** 1308–1315 (1951).
2. S. C. R. Dennis, S. N. Singh and D. B. Ingham, The steady flow due to a rotating sphere at low and moderate Reynolds numbers, *J. Fluid Mech.* **101,** 257–279 (1980).
3. W. S. Amato and C. Tien, Free convection heat transfer from isothermal spheres in water, *Int. J. Heat Mass Transfer* **15,** 327–338 (1972).
4. L. Pera and B. Gebhart, Experimental observations of wake formation over cylindrical surface in natural convection flows, *Int. J. Heat Mass Transfer* **15,** 175–177 (1972).
5. J. H. Merkin, Free convection boundary layers on cylinders of elliptic cross section, *J. Heat Transfer* **99,** 453–457 (1977).
6. L. S. Yao and S. A. Berger, Entry flow in a curved pipe, *J. Fluid Mech.* **67,** 177–196 (1975).
7. K. Stewartson, T. Cebeci and K. C. Chang, A boundary-layer collision in a curved duct, *Q. Jl Mech. Appl. Math.* **33,** 59–75 (1980).
8. K. Stewartson and C. J. Simpson, On a singularity initiating a boundary-layer collision, *Q. Jl Mech. Appl. Math.* **35,** 1–16 (1982).
9. L. S. Yao, Entry flow in a heated tube, *J. Fluid Mech.* **88,** 465–483 (1978).
10. A. F. Messiter, The vertical plate in laminar free convection, *J. Appl. Math. Phys. (ZAMP)* **27,** 633–651 (1976).
11. F. T. Smith and P. W. Duck, Separation of jets or thermal boundary layers from a wall, *Q. Jl Mech. Appl. Math.* **30,** 143–156 (1977).
12. K. T. Yang, Laminar free-convection wake above a heated vertical plate, *J. Appl. Mech.* **31,** 131–138 (1964).
13. K. Stewartson, On the flow near the trailing edge of a flat plate II, *Mathematika* **16,** 106–121 (1969).
14. A. F. Messiter, Boundary-layer flow near the trailing edge of a flat plate, *SIAM J. Appl. Math.* **18,** 241–257 (1970).
15. F. T. Smith, A note on a wall jet negotiating a trailing edge, *Q. Jl Mech. Appl. Math.* **31,** 473–479 (1978).
16. R. Yang and L. S. Yao, Natural convection along a finite vertical plate, *J. Heat Transfer* **109,** 413–418 (1987).
17. J. H. Merkin and F. T. Smith, Free convection boundary layers near corners and sharp trailing edge, *J. Appl. Math. Phys. (ZAMP)* **33,** 36–52 (1982).
18. L. S. Yao, A note on Prandtl's transposition theorem, *J. Heat Transfer* (1988), in press.
19. S. Goldstein, Concerning some solutions of the boundary-layer equations in hydrodynamics, *Proc. Camb. Phil. Soc.* **26,** 1–30 (1929).
20. L. S. Yao, Natural convection along a vertical wavy surface, *J. Heat Transfer* **105,** 465–468 (1983).

UNE FAIBLE COLLISION DE DEUX COUCHES LIMITES DE CONVECTION NATURELLE

Résumé—La collision de deux couches limites de convection naturelle à l'extrémité d'un coin vertical est considérée pour montrer qu'une structure d'écoulement à double couverture fournit une description convenable du mécanisme de convection qui est concerné par des problèmes de convection avec des changements brusques de géométrie. La présente théorie diffère des travaux précédents qui indiquent l'existence de régions d'écoulement à recirculation. Cette différence est due au fait que les structures d'écoulement recirculantes n'existent que pour les écoulements forcés, mais pas pour les couches limites de convection naturelle ou les jets pariétaux. La solution est obtenue ici par une application appropriée du théorème de transposition de Prandtl pour les géométries avec des déplacements finis de solide et elle convient aux couches limites ascendantes de convection naturelle et au panache thermique descendant. L'interaction du développement local de pression dans la couverture principale (couche externe) et du déplacement de la couverture basse (couche interne) déplace la singularité associée aux équations de la couche limite vers l'endroit où les couches visqueuses quittent la surface solide.

EIN SCHWACHER ZUSAMMENSTOSS DER GRENZSCHICHTEN ZWEIER NATÜRLICHER KONVEKTIONSSTRÖMUNGEN

Zusammenfassung—Der Zusammenstoß der Grenzschichten zweier natürlicher Konvektionsströmungen an der Spitze eines senkrechten Keils wird benutzt um zu zeigen, daß eine zweilagige Strömungsstruktur eine geeignete Beschreibung des Wärmetransports durch natürliche Konvektion und vieler Strömungsprobleme mit plötzlich wechselnder Geometrie erlaubt. Die vorgestellte Theorie unterscheidet sich von früheren Arbeiten, die auf die Existenz von Rückströmgebieten schließen lassen. Dabei wurde völlig vergessen, daß Rückströmungen nur in erzwungenen, nicht jedoch in der Grenzschicht natürlicher Konvektionsströmungen oder bei Wandstrahlen auftreten können. Die hier vorgestellte Lösung wurde durch eine Anwendung des Prandtl'schen Überlagerungstheorems für Geometrien mit endlichen Versetzungen erhalten. Sie nähert die Grenzschicht stromaufwärts und die Auftriebsfahne stromabwärts in geeigneter Weise an. Die Wechselwirkung zwischen dem örtlichen Druck in der Hauptebene (der äußeren Schicht) und der Verlagerung der unteren Ebene (der inneren Schicht) hebt die Singularität in den Grenzschichtgleichungen dort auf, wo die Grenzschicht die feste Oberfläche verläßt.

СЛАБОЕ ВЗАИМОДЕЙСТВИЕ ДВУХ СВОБОДНОКОНВЕКТИВНЫХ ПОГРАНИЧНЫХ СЛОЕВ

Аннотация—На примере взаимодействия двух свободноконвективных пограничных слоев вблизи вершины вертикально расположенного клина показано, что с помощью двухслойной структуры потока можно описывать механизм конвективного теплообмена во многих задачах конвекции с резким изменением геометрии. Данная теория отличается от предложенной ранее, которая указывала на наличие областей с рециркуляцией потока. Это отличие возникло из-за нежелания признать тот факт, что рециркуляционные потоки могут иметь место только при вынужденном течении, но не в свободноконвективных пограничных слоях или пристенных струях. Настоящее решение получено благодаря использованию транспозиционной теоремы Прандтля для приграничных областей и хорошо описывает восходящие свободноконвективные пограничные слои и опускные потоки в тепловом факеле. Связь между процессами изменения местного давления в основном слое (наружный) и перемещения нижнего слоя (внутренний) устраняет сингулярность в уравнениях пограничного слоя для области стекания вязких слоев с твердой поверхности.